A Five-Level Common Grounded Boost Inverter Topology with Model Predictive Control For Grid-Tied Photovoltaic Generation

Mokhtar Aly, Samir Kouro, Emad M. Ahmed, Thierry Meynard, Jose Rodriguez

A Five-Level Common Grounded Boost Inverter Topology with Model Predictive Control For Grid-Tied Photovoltaic Generation

Mokhtar Aly[1], Samir Kouro[2], Emad M. Ahmed[3,4], Thierry A. Meynard[5], José Rodriguez[6]

[1]*Facultad de Ingeniería y Tecnología, Universidad San Sebastián*, Bellavista 7, Santiago, Chile
[2] *Electronics Engineering Department, Universidad Tecnica Federico Santa Maria*, Valparaiso 2390123, Chile
[3]*Electrical Engineering Department, Aswan University*, Aswan 81542, Egypt
[4] *Department of Electrical Engineering, Jouf University, College of Engineering*, Sakaka 2014, Saudi Arabia
[5] *Institut National Polytechnique de Toulouse, University of Toulouse*, Toulouse, France
[6] *Universidad Andres Bello*, Santiago, Chile
mokhtar.aly@aswu.edu.eg, samir.kouro@ieee.org, emad@eng.aswu.edu.eg
thierry.meynard@laplace.univ-tlse.fr, jose.rodriguez@unab.cl

***Abstract*—This paper presents a new common grounded (CG) multilevel boost inverter (MI) topology for single-phase grid-tied photovoltaic (PV) applications. The proposed topology has the capability to fully eliminate the leakage currents in PV systems due to the using of the CG connection. Additionally, the proposed topology benefits the high boosting factor capability of the low PV voltage. The proposed topology represents a single stage power conversion system with reduced power components compared to the traditional two-stage PV power conversion systems. In addition, model predictive controller (MPC) is proposed in this paper to control the proposed topology. The proposed controller can control multiple objectives simultaneously without using cascaded controllers. The simulation results with the different case studies are provided. The results confirm the superiority of the proposed CG boost MI topology and the proposed MPC method. Furthermore, fast tracking of the grid active and reactive power demands is achieved using the proposed MPC method.**

***Index Terms*—common grounded (CG) inverter, model predictive controller (MPC), multilevel inverter (MI), photovoltaic (PV) applications.**

I. Introduction

Recently, wide concerns have been given for the leakage current issues in photovoltaic (PV) applications [1]. One of the feasible solutions for eliminating the leakage currents are the common ground (CG) inverter topologies [2]. In which, direct connection is achieved between the negative terminal at PV side with the neutral terminal at the grid side. Therefore, elimination of the common mode voltage (CMV) components and the leakage currents are obtained in accordance [3].

The CG topologies in the literature can be classified into inductor-based, capacitor-based, and impedance-based topologies [4]. Among them, the capacitor based topologies have shown superior performance regarding to the multilevel voltage output, reduced size, and reduced number of components. Several solutions have been presented in the literature using charge pump [5], virtual dc-link [6], and integrated two stages [7] topologies. Another solution based on the split source topology has been presented in [8], and its improved modulation method has been proposed in [9].

From another side, multilevel-based topologies have been introduced to benefit of the CG connection in addition to the multilevel voltage output. In [10], a five-level CG topology has been proposed using the flying capacitor leg. Another switched capacitor cell generalized multilevel inverter topology has been presented in [1]. However, these developed topologies can only buck the PV voltage and additional boosting stage is needed for low PV voltage applications. In [11], a six switch based boost inverter has been proposed for PV applications. The topology can achieve double boost of the input PV source with five-level output voltage. Another double boost switched capacitor topology has been presented in [12]. A triple boost topology has been presented in [13] for three phase applications. Additional high boost factor topology has been presented in [14]. However, these topologies suffer from the increased number of requires components, increased cost, and reduced efficiency.

Additionally, the control scheme represents a critical part in the development of CG PV solutions. The required cascaded PI controllers in CG topologies represent the main reason for the complexity of controller design in these topologies [15]. The model predictive control (MPC)-based control schemes have proven superior performance at achieving multiple objectives simultaneously with using a single objective function [16]. Recently, finite control set (FCS) MPC schemes have been applied for different CG-MI topology [17], and three port topologies [18].

Motivated by the aforementioned CG solutions, this paper presents a new boost MI topology with CG connection for PV applications. The main benefits of the proposed topology are the elimination of leakage currents, multilevel voltage output, high boosting factor, and reduced number of components. Additionally, MPC scheme is introduced for the proposed

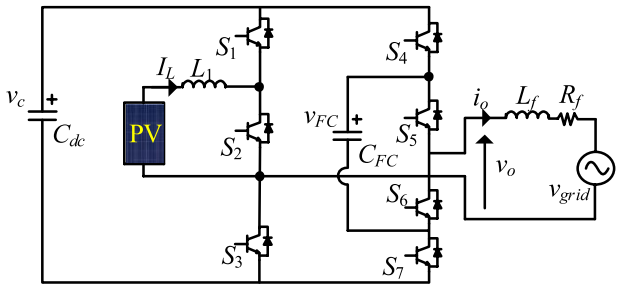

Fig. 1: The proposed CG boost MI PV topology.

TABLE I: The operating states of the proposed CG boost MI topology (1 is used for ON-state and 0 is used for OFF-state).

State	Output		Switch Signals						
	Level	v_o	S_1	S_2	S_3	S_4	S_5	S_6	S_7
1	v_{dc}	v_c	0	1	1	1	1	0	0
2	$0.5v_{dc}$	$v_c - v_{FC}$	0	1	1	1	0	1	0
3		v_{FC}	0	1	1	0	1	0	1
4		0	0	1	1	0	0	1	1
5	0	0	1	0	1	0	0	1	1
6		0	1	1	0	1	1	0	0
7	$-0.5v_{dc}$	$v_{FC} - v_c$	1	1	0	1	0	1	0
8		$-v_{FC}$	1	1	0	0	1	0	1
9	$-v_{dc}$	$-v_c$	1	1	0	0	0	1	1

topology to control the various currents and voltages in the proposed topology in addition to satisfying the grid demand requirements.

The remaining of the paper is organized as follows: Section II introduces the operation and switching states of the proposed CG topology. The proposed controller with its mathematical modelling are provided in Section III. Section IV presents the obtained simulation results of the proposed topology and MPC scheme. The conclusion is presented in Section V.

II. The Proposed Topology and Controller

A. The Proposed Topology

The power circuit of proposed CG boost topology is shown in Fig. 1. The topology is composed of seven power switches $S_1 \sim S_7$, an inductor L_1, flying capacitor C_{FC} and dc capacitor C_{dc}. The inductor of the PV side is employed with the capacitor C_{dc} to achieve boosting of the low PV voltage. Whereas, the flying capacitor is controlled to maintain half of the capacitor C_{dc} voltage ($v_{FC} = 0.5v_c = 0.5v_{dc}$). The proposed topology generates five different voltage levels ($v_{dc}, v_{dc}/2, 0, -v_{dc}/2, -v_{dc}$). The topology includes two different legs: The first leg includes the flying capacitor to generate the multilevel output, while the second leg includes the CG connection that achieves the elimination of leakage currents. In addition, the proposed topology has a reduced number of components compared to existing two stage and boost topologies in the literature.

B. The Inverter Switching States

The various switching states of the proposed CG boost MI topology are shown in Table. I. The outputted five-levels using the proposed topology have nine switching states, and some of them are redundant states. The table includes also the switching pulses for generating the five-voltage levels. In addition, the various states have different charging and discharging control actions of the inductor current and capacitor voltages.

III. The Proposed MPC Scheme

The control system has to control the capacitor C_{dc} voltage, the flying capacitor C_{FC} voltage, the inductor L_1 current and the injected grid current i_o at their reference values.

Fig. 2 shows the block diagram representation of the proposed controller. The slow-response outer loop is employed for controlling the capacitor voltage v_c at its reference value $v_{c,ref}$. The classical PI controller is usually employed in this loop. The output of the controller is used to develop the reference active power for the grid P_{grid}. Then, the reference injected grid current is evaluated using the reference active power P_{grid} and reactive power Q_{grid} as follows:

$$I_{L,ref}(k+1) = \frac{P_{grid}}{0.5V_{grid(peak)cos(\theta)}} sin(2\pi f_l t + \theta) \quad (1)$$

where, $V_{grid(peak)}$ represents the peak grid voltage, and θ is the power-factor angle. It is calculated using the reference active and reactive power of the grid as fallowing:

$$\theta = tan^{-1}\frac{Q_{grid}}{P_{grid}} \quad (2)$$

From the grid-side, the inverter output voltage v_o is related to the grid voltage v_{grid}, the injected grid-current i_o and the L-filter components (L_f and R_f) as follows:

$$v_o = v_{grid} + R_f i_o + L_f \frac{di_o}{dt} \quad (3)$$

Thence, the continuous-time modelling of grid current is expressed as follows:

$$\frac{di_o}{dt} = \frac{1}{L_f}(v_o - v_{grid} - R_f i_o) \quad (4)$$

Using Euler approximation method, the first-order derivative of injected grid current is written as follows:

$$\frac{di_o}{dt} = \frac{i_o(k+1) - i_o(k)}{T_s} \quad (5)$$

where T_s is the MPC sampling time period. While $(k+1)$ and (k) are the $(k+1)^{th}$ and $(k)^{th}$ sampling intervals of output inverter current. Based on (4) and (5), the grid output current is predicted for $(k+1)^{th}$ instant as follows:

$$i_o(k+1) = \frac{T_s}{L_f}(v_o(k) - v_{grid}(k)) + (1 - \frac{R_f T_s}{L_f}) i_o(k) \quad (6)$$

The output voltage of the proposed topology is dependant on the applied switching signals. The output voltage v_o can be predicted for the available states as follows:

$$v_o(k) = (S_4 + S_5)v_{FC}(k) - (S_1 + S_2 - 1)v_c(k) \quad (7)$$

Additionally, the control method has to preserve the current I_L through inductor L_1 at its reference value. The predicted current can be expressed as follows:

$$I_L(k+1) = I_L(k) + \frac{T_s}{L_1}V_{PV}(k) \quad (8)$$

where $i_L(k)$ is the measured current at the sampling instant k and $V_{PV}(k)$ is the measured voltage of PV side. However, the predicted current for state no. 5 can be expressed as follows:

$$I_L(k+1) = I_L(k) + \frac{T_s}{L_1}(V_{PV}(k) - v_c(k)) \quad (9)$$

The reference value for the inductor current $I_{L,ref}$ is determined by the MPPT controller as follows:

$$I_{L,ref}(k+1) = \frac{P_{PV}}{V_{PV}} \quad (10)$$

where P_{PV} is the MPPT power of the PV source.

The same procedures are utilized for predicting the capacitor C_{FC} voltage for the subsequent sampling instant $v_{FC}(k+1)$ as follows:

$$v_{FC}(k+1) = v_{FC}(k) + \frac{T_s}{C_{FC}}(S_4 - S_5)i_o(k) \quad (11)$$

Finally, the MPC scheme has to control the grid current, inductor current and the capacitor voltage according to their references. The currents and voltages are predicted for all the possible states in the proposed topology. The overall control scheme of the proposed topology is shown in Fig. 2. The MPC method employs a single objective function for controlling multiple elements, which represents a powerful benefit of the application of MPC methods. The objective function is evaluated for all possible switching states and it can be expressed as follows:

$$\begin{aligned} g(k) &= \lambda_1(i_{o,ref}(k+1) - i_o(k+1)) \\ &+\lambda_2(I_{L,ref}(k+1) - I_L(k+1)) \\ &+\lambda_3(v_{FC,ref}(k+1) - v_{FC}(k+1)) \end{aligned} \quad (12)$$

where λ_1, λ_2, and λ_3 are the weighting factor values for the inverter ac current, the inductor L_1 current and the capacitor C_{FC} voltage, respectively. The MPC method finally selects the state that achieves minimized cost function and hence better tracking for the references. The corresponding gating pulses according to Table I are outputted and applied to the seven power switches.

IV. Simulation Results

In this part, the proposed topology and MPC scheme are simulated and tested at various operating cases. The simulation parameters of the selected case are shown in Table. II. The PV source has an output voltage of 75V, which is much lower than the grid peak voltage. Hence, high step up of the voltage is essential, which is achieved by the proposed topology. The capacitor C_{dc} voltage is selected to be higher than the grid voltage peak and the voltage of the flying capacitor is selected to be half of v_c (v_{FC}=v_c/2).

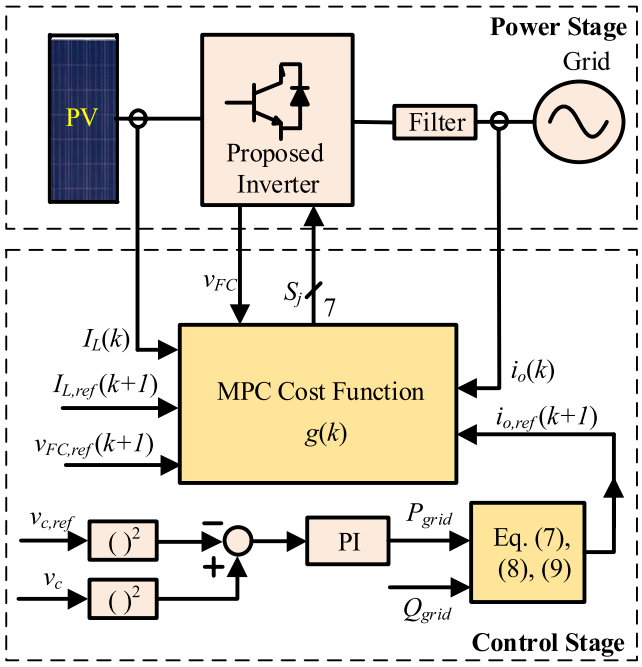

Fig. 2: Block diagram representation of the proposed MPC method.

TABLE II: Simulation parameters.

Parameter	Value
Input PV voltage V_{PV}	75V
Capacitor C_{dc} voltage v_c	400-430V
Capacitor C_{FC} voltage v_{FC}	200-215V
C_{dc} capacitance	2000μF
C_{FC} capacitance	1000μF
L_1 inductance	4.5mH
Grid line frequency f_l	50Hz
Grid peak-voltage	311V
Grid filter inductance L_f	3.5mH
Grid filter resistance R_f	50mΩ
Sampling frequency f_s $(= 1/T_s)$	50kHz

A. Case 1: Step-up in PV Power

In this case, a step change of the PV power from 1500W to 3000W is made. The reference current of the inductor L_1 is stepped in accordance from 20A to 40A. Fig. 3 shows the obtained simulation results in this case. It can be seen from Fig. 3a that the proposed topology generates five output voltage levels, which is considered beneficial in reducing the required grid filters. The current tracking response is shown in Fig. 3b. A sinusoidal current tracking is achieved and it is in phase with the grid voltage. Additionally, a smooth tracking of capacitor voltages at their reference values can be seen from Fig. 3c. The tracking of the current I_L is shown in Fig. 3d. It can be seen that a fast tracking is achieved using the proposed MPC scheme.

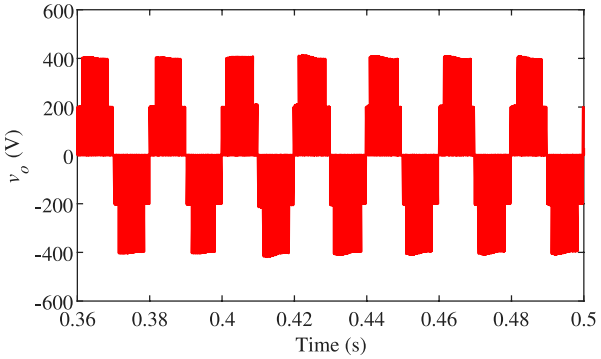

(a) Output voltage

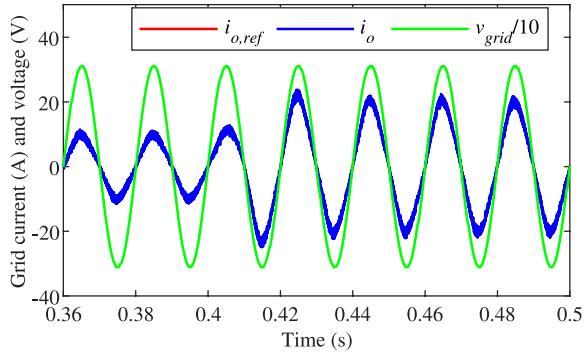

(b) Grid current tracking

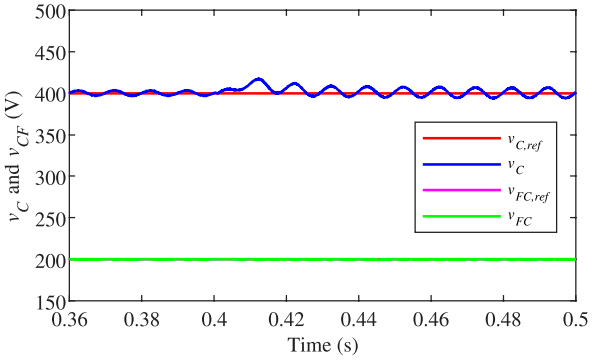

(c) Capacitor voltages tracking

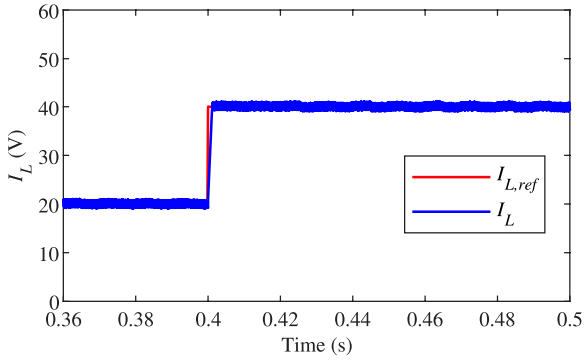

(d) Inductor current tracking

Fig. 3: Simulation results of case 1.

B. Case 2: Step Change in Capacitor Voltage References

In this case, a step change of the capacitor voltages is made. The reference voltage of capacitor C_{dc} is stepped from 400V to 420V and the reference of capacitor C_{FC} is stepped from from 200V to 210V. The corresponding results are shown in Fig. 4. It can be seen that the output voltage is preserved at five voltage levels and proper tracking of the grid current. Additionally, the capacitor voltages are preserved at their references with fast response. As there are no step change in the PV power, the inductor current is maintained at its reference value without interruption.

C. Case 3: Step-down in PV Power

In this case, a step change of the PV power from 3000W to 1125W has been made. The reference current of the inductor L_1 is reduced in accordance from 40A to 15A. Fig. 5 shows the obtained simulation results in this case. The results show the fast and accurate tracking of the currents and capacitor voltages. Additionally, sinusoidal grid current is achieved and five-level output voltage waveform is outputted by the proposed topology and inverter.

D. Case 4: Step Change in Grid Reactive Power

In this case, a step change of the injected grid reactive power from 0 VAR to -1500 VAR has been made. The reference grid current is estimated in accordance. The results of this case are shown in Fig. 6. It can be seen that the proposed topology and MPC scheme are capable of supporting the grid reactive power. The tracking of the grid current is achieved with fast tracking. Additional, high quality waveforms are obtained in this case. This, in turn, proves the feasibility and effectiveness of the proposed topology and control scheme.

V. Conclusions

A new topology has been proposed in this paper for grid-tied PV applications. The main benefits of the proposed topology are as follows: It employs the common ground connection, which leads to eliminate the leakage current components; It is capable of achieving high boosting factor of the low PV voltage to the grid level; It can generate five-level output voltage waveform; It employs low number of power switches and passive components; It represents a single stage power conversion system. Additionally, a model predictive controller (MPC) scheme is proposed for controlling the proposed topology. The proposed MPC scheme can control the various currents and voltages of the proposed topology using a single objective function, while helps at achieving fast and accurate tracking response. The obtained simulation results for the various operating cases have shown superior performance of the proposed topology and MPC scheme.

VI. Acknowledgments

This work was supported by ANID through projects SERC Chile (ANID/FONDAP15110019), AC3E (ANID/Basal/FB0008), FONDECYT 1191532, 11180233, ACT192013 and 1210208.

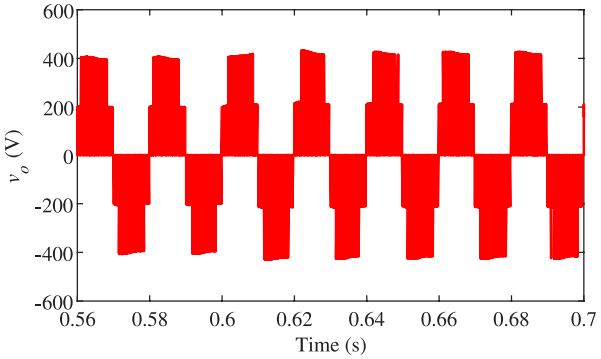

(a) Output voltage

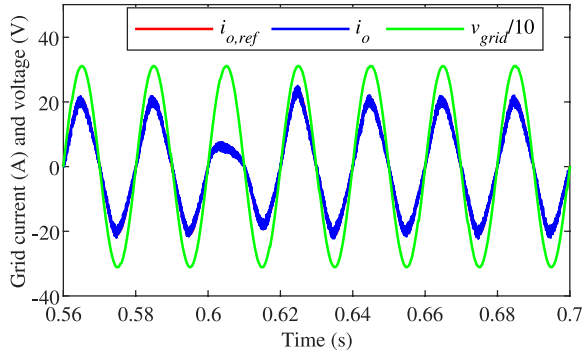

(b) Grid current tracking

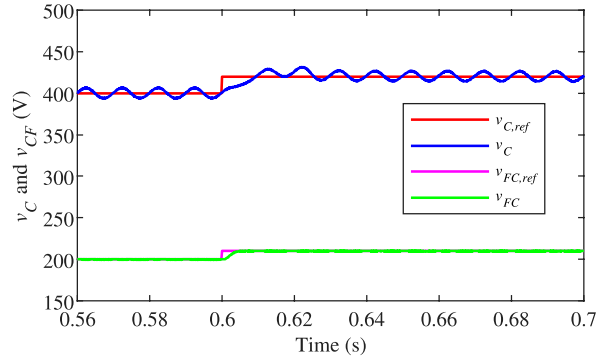

(c) Capacitor voltages tracking

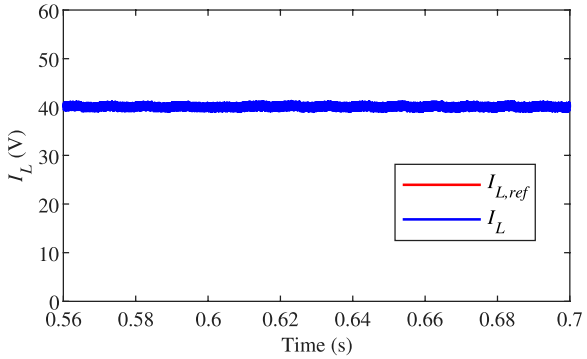

(d) Inductor current tracking

Fig. 4: Simulation results of case 2.

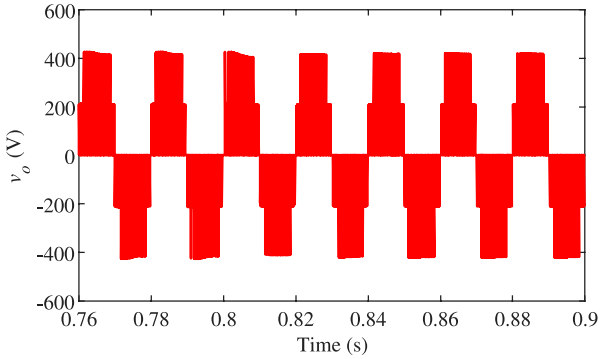

(a) Output voltage

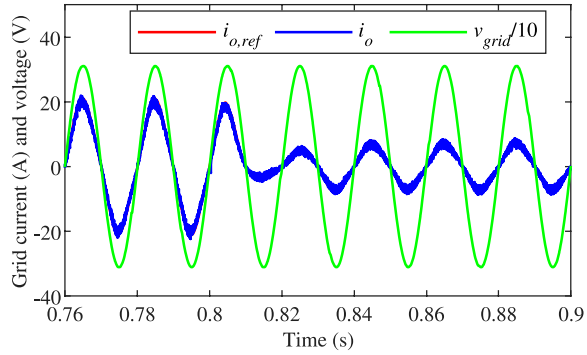

(b) Grid current tracking

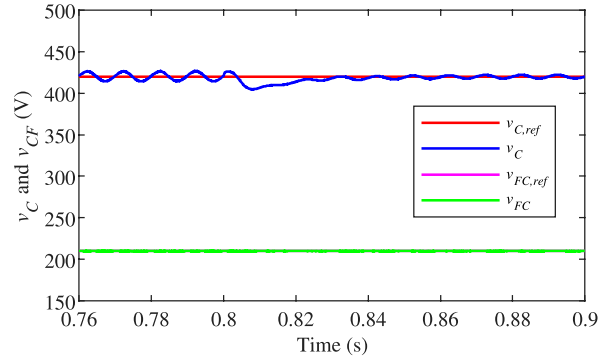

(c) Capacitor voltages tracking

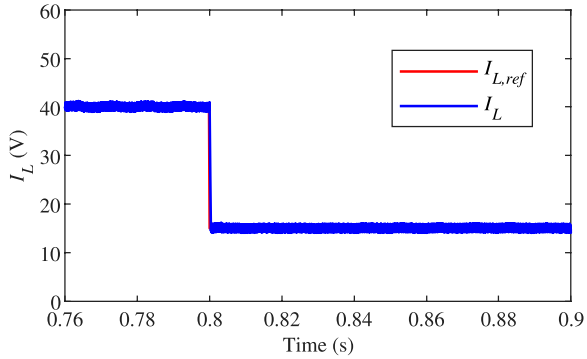

(d) Inductor current tracking

Fig. 5: Simulation results of case 3.

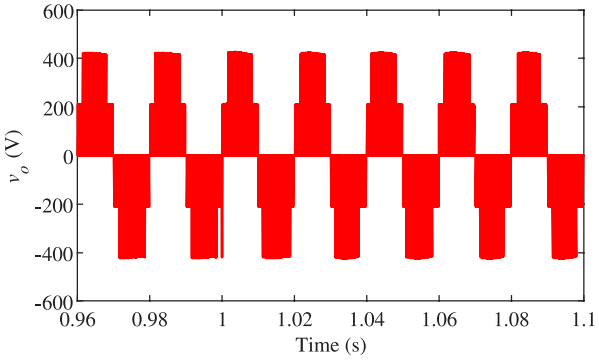

(a) Output voltage

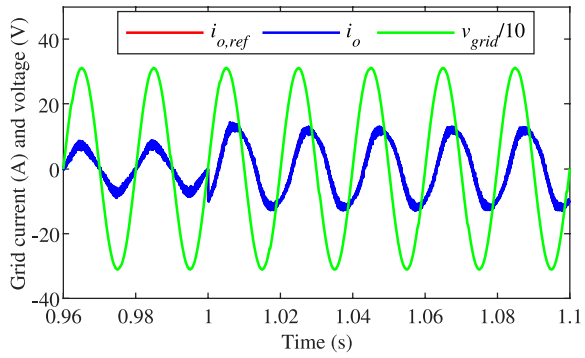

(b) Grid current tracking

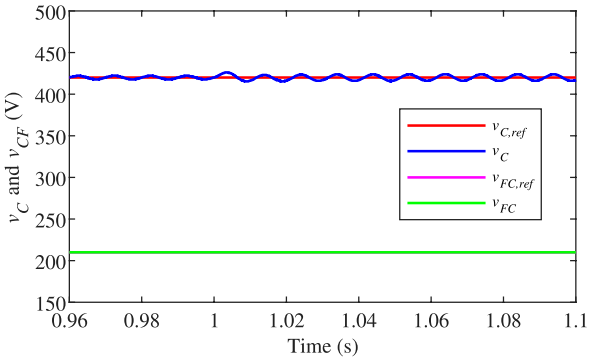

(c) Capacitor voltages tracking

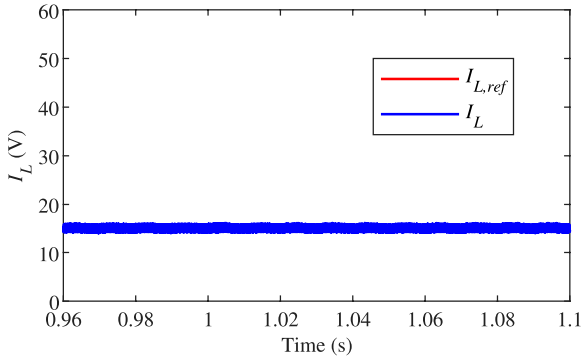

(d) Inductor current tracking

Fig. 6: Simulation results of case 4.

References

[1] A. Kadam and A. Shukla, "A multilevel transformerless inverter employing ground connection between pv negative terminal and grid neutral point," *IEEE Transactions on Industrial Electronics*, vol. 64, no. 11, pp. 8897–8907, 2017.

[2] M. Aly, F. Carnielutti, M. Norambuena, E. M. Ahmed, S. Kouro, and J. Rodriguez, "A finite control set-model predictive control method for step-up five level doubly grounded photovoltaic inverter," in *IECON 2020 The 46th Annual Conference of the IEEE Industrial Electronics Society*, 2020, pp. 4595–4600.

[3] M. Aly, C. A. Rojas, E. M. Ahmed, and S. Kouro, "Leakage current elimination pwm method for fault-tolerant string h-npc pv inverter," in *IECON 2019 - 45th Annual Conference of the IEEE Industrial Electronics Society*, vol. 1, 2019, pp. 6489–6494.

[4] A. Kadam and A. Shukla, "A multilevel transformerless inverter employing ground connection between pv negative terminal and grid neutral point," *IEEE Transactions on Industrial Electronics*, vol. 64, no. 11, pp. 8897–8907, 2017.

[5] J. F. Ardashir, M. Sabahi, S. H. Hosseini, F. Blaabjerg, E. Babaei, and G. B. Gharehpetian, "A single-phase transformerless inverter with charge pump circuit concept for grid-tied pv applications," *IEEE Transactions on Industrial Electronics*, vol. 64, no. 7, pp. 5403–5415, 2017.

[6] Y. Gu, W. Li, Y. Zhao, B. Yang, C. Li, and X. He, "Transformerless inverter with virtual DC bus concept for cost-effective grid-connected PV power systems," *IEEE Transactions on Power Electronics*, vol. 28, no. 2, pp. 793–805, Feb. 2013.

[7] N. Vazquez, J. Vazquez, J. Vaquero, C. Hernandez, E. Vazquez, and R. Osorio, "Integrating two stages as a common-mode transformerless photovoltaic converter," *IEEE Transactions on Industrial Electronics*, vol. 64, no. 9, pp. 7498–7507, Sep. 2017.

[8] X. Hu, P. Ma, B. Gao, and M. Zhang, "An integrated step-up inverter without transformer and leakage current for grid-connected photovoltaic system," *IEEE Transactions on Power Electronics*, vol. 34, no. 10, pp. 9814–9827, Oct. 2019.

[9] S. S. Lee, Y. P. Siwakoti, C. S. Lim, and K.-B. Lee, "An improved PWM technique to achieve continuous input current in common-ground transformerless boost inverter," *IEEE Transactions on Circuits and Systems II: Express Briefs*, vol. 67, no. 12, pp. 3133–3136, Dec. 2020.

[10] F. B. Grigoletto, "Five-level transformerless inverter for single-phase solar photovoltaic applications," *IEEE Journal of Emerging and Selected Topics in Power Electronics*, pp. 1–1, 2019.

[11] R. Barzegarkhoo, Y. P. Siwakoti, N. Vosoughi, and F. Blaabjerg, "Six-switch step-up common-grounded five-level inverter with switched-capacitor cell for transformerless grid-tied PV applications," *IEEE Transactions on Industrial Electronics*, vol. 68, no. 2, pp. 1374–1387, Feb. 2021.

[12] R. Barzegarkhoo, Y. P. Siwakoti, and F. Blaabjerg, "A new switched-capacitor five-level inverter suitable for transformerless grid-connected applications," *IEEE Transactions on Power Electronics*, vol. 35, no. 8, pp. 8140–8153, Aug. 2020.

[13] M. Chen, P. C. Loh, Y. Yang, and F. Blaabjerg, "A six-switch seven-level triple-boost inverter," *IEEE Transactions on Power Electronics*, vol. 36, no. 2, pp. 1225–1230, 2021.

[14] M. Chen, Y. Yang, P. C. Loh, and F. Blaabjerg, "A single-source nine-level boost inverter with a low switch count," *IEEE Transactions on Industrial Electronics*, pp. 1–1, 2021.

[15] Y. Xia, J. Roy, and R. Ayyanar, "A capacitance-minimized, doubly grounded transformer less photovoltaic inverter with inherent active-power decoupling," *IEEE Transactions on Power Electronics*, vol. 32, no. 7, pp. 5188–5201, 2017.

[16] M. Aly, F. Carnielutti, M. Norambuena, S. Kouro, and J. Rodriguez, "A model predictive control method for common grounded photovoltaic multilevel inverter," in *IECON 2020 The 46th Annual Conference of the IEEE Industrial Electronics Society*, 2020, pp. 2401–2406.

[17] M. Aly, F. Carnielutti, M. Norambuena, E. M. Ahmed, S. Kouro, and J. Rodriguez, "Fixed switching frequency model predictive controller for doubly-grounded five-level photovoltaic inverter," in *ECCE-Asia 2021 The IEEE Energy Conversion Congress and Exposition – Asia, 2021*, 2021, pp. 1–6.

[18] S. Neira, J. Pereda, and F. Rojas, "Three-port full-bridge bidirectional converter for hybrid DC/DC/AC systems," *IEEE Transactions on Power Electronics*, vol. 35, no. 12, pp. 13 077–13 084, Dec. 2020.